

A Swift Response to Newly Discovered, Nearby Transients [†]

Peter J. Brown ^{1,2,*} , Macie Robertson ² , Yaswant Devarakonda ^{1,2} , Emily Sarria ³, David Pooley ^{4,5} 
and Maximilian D. Stritzinger ⁶ 

¹ Mitchell Institute for Fundamental Physics and Astronomy, College Station, TX 77843, USA

² Department of Physics and Astronomy, Texas A&M University, 4242 TAMU, College Station, TX 77843, USA

³ Department of Math, Texas A&M University, 3368 TAMU, College Station, TX 77843, USA

⁴ Department of Physics and Astronomy, Trinity University, San Antonio, TX 78212, USA

⁵ Eureka Scientific, Inc., Oakland, CA 94602, USA

⁶ Department of Physics and Astronomy, Aarhus University, Ny Munkegade 120, DK-8000 Aarhus C, Denmark

* Correspondence: pbrown@physics.tamu.edu

[†] Based on observations by the Neil Gehrels Swift Observatory Guest Investigator Key Project.

Abstract: The Neil Gehrels Swift Observatory has proven to be an extraordinary supernova (SN) observatory. The clearest application of Swift's unique strengths is obtaining very early UV and X-ray data of young SNe, which enables robust constraints on their progenitor systems. As part of a year-long Swift Guest Investigator Key Project, we initiated a follow-up program to rapidly observe all of the nearest (distance < 35 Mpc or roughly $z < 0.008$) extragalactic transients without waiting for them to be spectroscopically classified as supernovae. Among the possible results were to measure any UV-bright radiative cooling following the shock breakout from core-collapse SNe and shock emission from the interaction of thermonuclear Type Ia SNe with a non-degenerate companion. Just as importantly, uniformly following up and analyzing a significant sample can constrain the fraction of events for which the shock emission is not seen. Here we present the UV and X-ray measurements performed during our campaign. Our sample of 24 observed triggers included three SNe Ia, six SNe II, three stripped-envelope, core-collapse SNe, five galactic transients, three extragalactic SN imposters, and four unconfirmed transients. For our sample, the median delay time from the discovery image to the first Swift image was 1.45 days. We tabulate the X-ray upper limits and find they are sufficiently deep to have detected objects as X-ray luminous as GRB060218/SN2006aj. Other X-ray-detected SNe such as SNe 2006bp, 2008D, and 2011dh would have been detectable in some of the observations. We highlight the spectroscopically classified Type II SN 2018hna with UV-optical light curves indicating a luminosity and flux evolution very similar to SN 1987A.

Keywords: time domain astronomy (2109); transient sources (1851); supernovae (1668); ultraviolet astronomy(1736); ultraviolet Telescopes (1743); ultraviolet transient sources (1854); X-ray detectors (1815); X-ray observatories (1819); X-ray telescopes (1825); X-ray transient sources (1852)



Citation: Brown, P.J.; Robertson, M.; Devarakonda, Y.; Sarria, E.; Pooley, D.; Stritzinger, M.D. A Swift Response to Newly Discovered, Nearby Transients. *Universe* **2023**, *9*, 218. <https://doi.org/10.3390/universe9050218>

Academic Editors: Ezio Caroli, Peter Roming and Michael Siegel

Received: 7 January 2023

Revised: 24 March 2023

Accepted: 28 March 2023

Published: 3 May 2023



Copyright: © 2023 by the authors. Licensee MDPI, Basel, Switzerland. This article is an open access article distributed under the terms and conditions of the Creative Commons Attribution (CC BY) license (<https://creativecommons.org/licenses/by/4.0/>).

1. A Prompt, Volume-Limited Transient Follow-Up Program with Swift

The Neil Gehrels Swift Observatory [1] began observing SNe in 2005 [2]. Since then, it has observed approximately 1000 SNe, including all major classes and subtypes (see [3]). Most of those SNe were targets of a campaign to study the temporal evolution of the UV flux with the Swift Ultraviolet/Optical Telescope (UVOT; [1,4]). Because they are co-pointed, there is a comparable rise in the number of SNe observed in the X-rays with Swift's X-Ray Telescope (XRT; [5]). Though most SNe are not detected in X-rays, Swift XRT has contributed significantly to the number of SNe with X-ray detections, as well as significant limits on the X-ray production from many others (e.g., [6–10]). This explosion of data represents an order of magnitude increase in the number of SNe observed in the UV and X-ray compared to earlier missions.

With a few notable exceptions—the GRB-SN 2006aj [11] and the shock breakout of SN 2008D [12]—SNe are not routinely discovered in the Swift data. Swift supernova observations rely on a SN being discovered by ground-based telescopes, announced, and submitted as a Target of Opportunity (ToO) request to Swift. The one-by-one nature of Swift ToOs tends to create a sample full of bias and selection effects as well as delay the time of the first observation. Bright or peculiar objects are often immediately pounced on. Fainter objects might be delayed while waiting for a spectroscopic classification to see if it is the type in which a particular group is interested. Swift GI programs typically have a narrow focus to observe SNe from a particular subclass or host galaxy type. For better or worse, criteria for new targets have evolved with experience as we learn the UV brightness, scientific utility, and observability of different SN types [13].

With modern, wide-field SN surveys such as the Palomar Transient Facility (PTF; [14,15]), All Sky Automated Survey for SuperNovae (ASAS-SN; [16]), the Asteroid Terrestrial-impact Last Alert System (ATLAS; [17]), the Distance-Less-Than 40 Mpc SN search (DLT40; [18]), Catalina Real-Time Transient Survey [19], Gaia Science Alerts [20], the Young Supernova Experiment (YSE; [21]), and the Zwicky Transient Facility (ZTF; [22]), in addition to individuals and small teams' diligent efforts (e.g., [23–25]), the whole visible sky is being covered every few nights. That means that new, nearby transients are almost always brightening above the limiting magnitude just a few days after explosion. For very nearby SNe, this means a few days after explosion (see e.g., [26]). These developments made it timely to pursue a rapid, type-blind follow-up campaign of all nearby SNe. An unbiased sample is an important comparison with the bulk properties of the whole Swift sample.

Most critically, pursuing SNe immediately after discovery/announcement rather than waiting for a spectroscopic type also narrows the gap between explosion and the first Swift observation. Swift's rapid response capability allows newly discovered SNe to be observed within hours of announcement. This is important for SNe because the UV-bright shock breakout of core-collapse SNe (e.g., [27]) or the expected UV flux from the interaction of the ejecta from a SN Ia colliding with a companion star (e.g., [28,29]) will fade in just a matter of days. Type II SNe begin very hot and UV-bright, but rapidly cool and fade [30,31]. Early observations of SN 2011fe showed how the constraints on the companion size are weakened for every day of delay [32]. Swift's fast response has led to unprecedented early-time UV data.

Constraining Type Ia SN interactions and the shock breakouts of core-collapse SNe motivated the depth of the observing program described in this paper. As shown in Figure 1, an absolute magnitude of $uvw1 \sim -13$ would detect all of the SNe Ia with UV flux excesses and most of the early fading seen in stripped-envelope core-collapse SNe. A modest combined exposure time of 3000 s using the UV-weighted UVOT mode 0x223f gives a limiting magnitude of $uvw1 \sim 20$. This results in a distance limit of ~ 35 Mpc. The proposed Swift Guest Investigator Key Project was over a two year period to observe every extragalactic transient within 35 Mpc for three observations (with a daily cadence) for 3 ks. One year was approved. This paper summarizes the results of that one-year project.

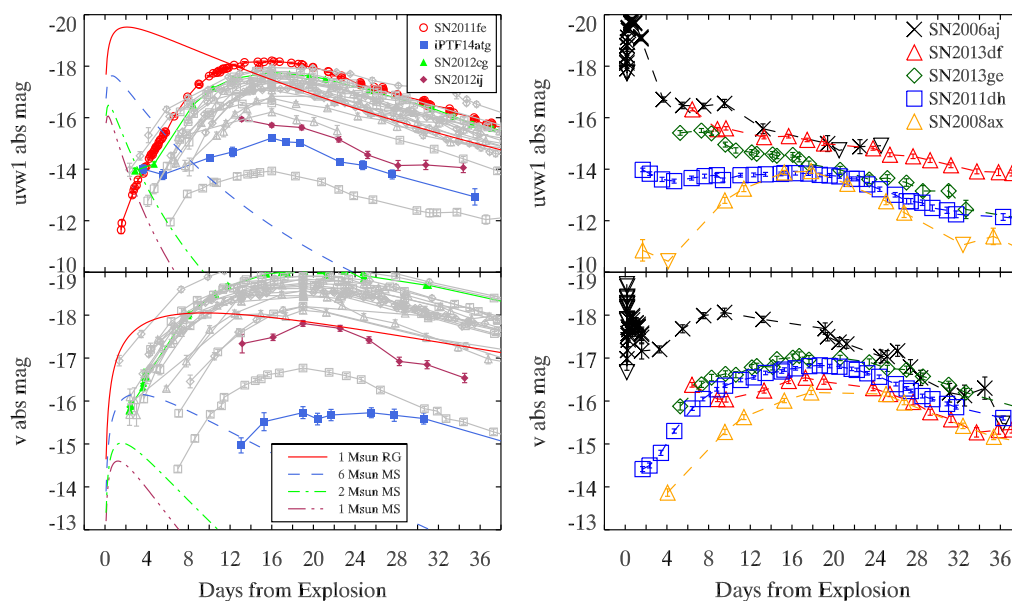


Figure 1. Left panel: Absolute magnitudes of Swift Type Ia SNe in the near-UV *uvw1* band and the optical *v* band (accounting for distance but not reddening in the observations). Highlighted are SN 2011fe and three candidates with an early UV excess (iPTF14atg; [33]; SN 2012cg; [34]; SN 2012ij; found during the creation of SOUSA). Although solar-type main sequence stars are predicted to be too faint to constrain, early Swift observations can rule out red giant and six solar mass main sequence star companions. The upper and lower panels show how much more powerful the UV is than the optical for constraining the companion from shock interaction. **Right panel:** Absolute magnitudes of some stripped-envelope core-collapse SNe observed in the near-UV *uvw1* band and the optical *v* band (accounting for distance but not reddening in the observations) which appear to show UV emission from a shock breakout or the subsequent adiabatic cooling. Only the objects with the brightest UV shocks have detectable excesses in their early optical light curves. These plots motivated the target magnitude of -13 in the *uvw1* filter.

2. Swift Observations

2.1. Triggering on New Candidates

Newly discovered transients were monitored using e-mailed notifications of reports and classifications from the Transient Name Server (TNS¹). Observations were requested for new transients if they met the 35 Mpc distance criteria. The resulting sample is distance limited but not distance complete; i.e., transients in the direction of the Sun would not be discovered or followed up by this program. Distances were generally evaluated based on the nearest galaxy with a redshift in the NASA Extragalactic Database (NED), while SN 2018ilu was triggered because the spectroscopic redshift of the SN was given as 0.007 [35]. Two transients turned out to be more distant objects near a foreground galaxy within our distance criteria, and at least three were galactic transients along the line of sight to a nearby galaxy. This was preferred to missing objects or critical early observations.

Our goal was a distance-limited, unbiased—not necessarily pure—sample, so we triggered (i.e., requested Swift ToO observations as part of this GI program) on an object if it could be a young SN in a nearby galaxy. This resulted in observations of some objects which were not young, nearby SNe. These are further discussed in Section 2.3.

Three observations of duration 3000 s each with a cadence of one day were requested as part of this program. We requested UVOT mode 0x0270 for observations uploaded directly to the spacecraft as an automatic target (AT) and 0x223f for observations that could be scheduled in the pre-planned science timeline (PPST). UVOT mode 0x0270 executes the following sequence of filters with the given exposure times, designed to use all six filters in a 1000 s single-orbit snapshot with any extra time being used in the uvm2 filter: uvw1 (270 s), u (130 s),

b (130 s), uvw2 (540 s), v (130 s), uvm2 (3000 s). This sequence would likely be repeated over 2-4 orbits in separate snapshots (limited by observing constraints and target priority) until the requested observing time is completed. This mode is requested for AT observations because most of the modes scale the exposure times in each filter based on the snapshot length which may not be accurately known for an AT observation, resulting in missed filters if the snapshot is shorter than the calculated time. Requested for pre-planned observations, UVOT mode 0x223f divides the observing time in each snapshot using the following sequence and ratios: uvw1 (600), u (200), b (200), uvw2 (1000), v (200 s), uvm2 (1600). XRT observations used the photon counting (PC) mode to create an image. For some of the objects, further observations (beyond the pre-approved three) were requested by ourselves or others. The objects triggered on and observed by Swift are tabulated in Table 1.

2.2. Time from Discovery to Swift Observation

The time delay between the explosion and the beginning of the Swift observation is composed of several different actions which are controlled by different groups and have different strategies to minimize. To give a snapshot in time of the responsiveness of Swift, Table 1 includes the time of the discovery, and the times (in days) between the previous non-detection (when reported) and the discovery, the discovery and the report to the Transient Name Server (TNS), the time delay between the report and the ToO submission, and the ToO submission and the beginning of the observation. The cadence of the survey (or time between deep visits of different surveys) determines the maximum time between the explosion being detectable and first being observed by a survey. The delay between the time of the image in which the transient is discovered to the time it is reported requires image processing, transient identification, and TNS submission. The time between the TNS report and the Swift ToO submission in this program involved the PI or collaborator seeing the e-mailed report, verifying the observability with Swift, and submitting the ToO form. The Swift observation delay involves the receipt of the request by the Swift Observatory Duty Scientist, approval of the PI, and the scheduling of the observation given observing constraints and the existing Swift plan.

Figure 2 shows histograms of these different delay times, while Figure 3 shows timelines of those delays added together. As shown, the delays at each stage are comparable, about 0.5 days. The largest obstacle that increases the (unknown) time delay between explosion and observation is the time between observations to discover the SNe. This is harder to quantify for this sample due to many of the previous non-detections not being reported. Shortening the cadence between SN search visits, rapidly identifying new transients in those images, reporting them promptly, reducing the delay in submitting ToOs, and uploading new targets to Swift are the means to shorten the total delay. When humans are in the loop, the steps are most often delayed by the timing of work hours.

We focus here on the delay between the discovery and the Swift observations because those have delays we can measure. The physically important parameter is the delay between the SN explosion and the Swift observations. We do not know when the SNe exploded, but the time delay between the previous non-detection and the discovery is reported in Table 1. Recent non-detection puts a limit on the time since explosion, but the lack thereof does not mean a transient is not young. Therefore, we did not use this as criteria. A program focused solely on the youngest SNe, however, could have a constraint on the last non-detection to require it to be young. This would be best done with forced photometry from other surveys which might fill in the gap between the discovery image and the last non-detection by the discovery survey.

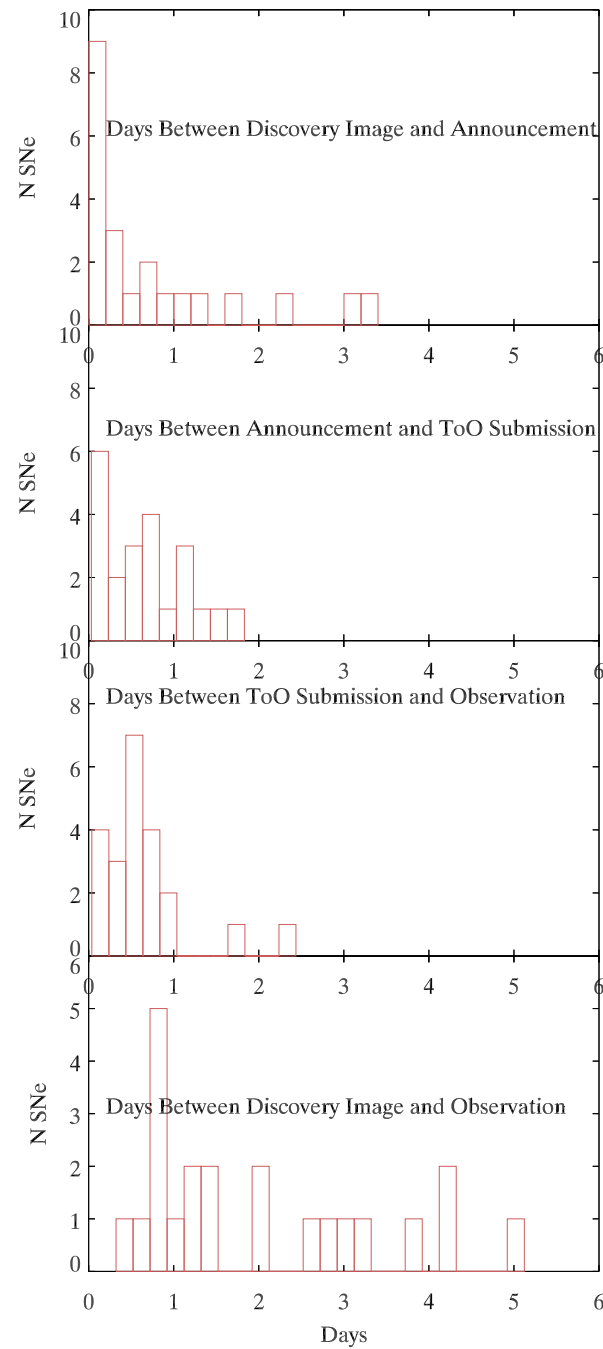


Figure 2. **Top:** Delay between the discovery image and the discovery report to TNS. The median delay was 0.3 days and the average 0.8 days. **Second:** Delay between the discovery report and the ToO submission time. The median delay was 0.5 days and the average 0.7 days. **Third:** Delay between the ToO submission and the start of Swift observations. The median delay was 0.5 days and the average 0.6 days. **Bottom:** The combined time delay from the discovery image to the first Swift observation. The median total delay was 1.4 days and the average 2.0 days.

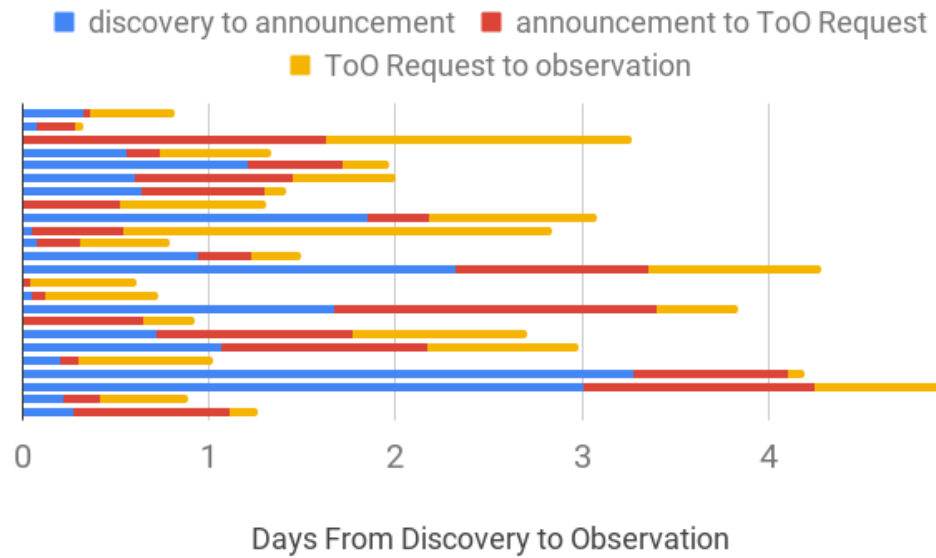


Figure 3. Graphical display of the delays between discovery and observation. The median total response time from discovery to Swift observation was 1.4 days and the average 2.0 days.

Table 1. Transient Targets Triggered on and Observed by Swift.

Name	R.A. (hh:mm:ss.ss)	Decl. (dd:mm:ss.ss)	Discoverer	Ref. ^a	Non-Det ^b (days)	Optical Detection (m/d/year h:m:s)	TNS ^c (days)	ToO ^d (days)	Obs ^e (days)
SN2018aoq	12:10:38.22	+39:23:47.87	LOSS	[36]	2.98	04/01/2018 10:21:29	0.33	0.03	0.45
SN2018apl	13:45:03	−41:52:23	ASASSN	[37]	6.05	04/03/2018 07:41:44	0.08	0.21	0.04
SN2018aoz	11:51:01.81	−28:44:38.69	DLT40	[38]	3.68	04/02/2018 07:24:57	0.005	1.62	1.64
AT2018avo	12:15:01.82	+33:10:38.40	Camarasa	[25]		04/16/2018 22:08:43	0.56	0.18	0.59
SN2018bbl	22:56:54.58	−37:20:22.27	BOSS	[39]	9.98	04/24/2018 03:54:13	1.20	0.51	0.26
AT2018bsk	12:28:51.62	−01:56:05.28	SNhunt	[40]	22.97	05/16/2018 05:08:25	0.60	0.85	0.55
AT2018bvt	12:22:39.60	+06:40:01.92	SNhunt	[41]	9.86	05/21/2018 04:06:53	0.64	0.66	0.12
AT2018bwo	00:14:01.72	−23:11:35.84	DLT40	[42]	6.58	05/22/2018 22:16:19	0.002	0.52	0.78
SN2018evk	23:15:45	+6:54:39.7	ATLAS	[43]	1.975	08/08/2018 14:06:43	1.85	0.33	0.89
SN2018gwo	12:08:38.82	+68:46:44.47	Wiggins	[23]	1.00	09/28/2018 02:41:31	0.04	0.50	2.30
SN2018hna	12 26 12.07	+58:18:50.8	Itagaki	[24]	20.88	10/22/2018 19:33:07	0.07	0.23	0.48
AT2018hrq	01:09:26.32	+35:42:39.01	LOSS	[44]	3.99	10/31/2018 08:54:27	0.94	0.29	0.26
AT2018hso	11:33:52	+53:07:07.42	ZTF	[45]	0.05	10/31/2018 12:51:50	2.32	1.04	0.93
AT2018htr	00:14:07.96	−23:10:09.71	DLT40	[46]	2.95	11/03/2018 23:43:48	0.002	0.04	0.57
SN2018imf	12:42:41.39	+13:15:54.83	Itagaki	[47]	105.38	11/14/2018 20:46:50	0.05	0.07	0.61
SN2018ilu	23:33:20.97	+04:48:34.74	ATLAS	[48]	1.97	11/12/2018 08:48:28	1.67	1.72	0.44
SN2018ivc	02:42:41.28	−00:00:31.92	DLT40	[49]	4.96	11/24/2018 01:47:09	0.002	0.65	0.27
SN2018lei	02:33:34.40	−39:02:45.24	ASASSN	[50]	4.31	12/31/2018 03:36:00	0.72	1.05	0.93
AT2019bl	07:04:35.67	+17:34:10.67	ATLAS	[51]	1.97	01/02/2019 11:03:50	1.07	1.10	0.81
SN2019np	10:29:21.98	+29:30:38.30	Itagaki	[52]	1.07	01/09/2019 15:57:35	0.20	0.10	0.72
SN2019yz	15:41:57.30	+00:42:39.45	ZTF	[53]	9.97	01/20/2019 12:23:02	3.27	0.83	0.10
AT2019abn	13:29:42	+47:11:16.99	ZTF	[54]	3.0	01/22/2019 13:19:43	3.00	1.25	0.77
AT2019ahd	10:51:12	+05:50:31.31	ATLAS	[55]	1.98	01/29/2019 12:27:21	0.22	0.19	0.48
AT2019clr	13:05:43.10	+37:37:36.12	SNhunt	[56]	24.11	03/28/2019 11:19:34	0.28	0.79	0.19

^a Discovery reference. ^b Time between the last reported non-detection and the image in which the SN was first detected. ^c Time between the image in which the transient was discovered and the discovery report was sent to TNS. ^d Time between the TNS discovery report and the submission of a Swift ToO request. ^e Time from ToO request to the start of Swift observations.

2.3. Supernova Type Distribution

The volumetric and fractional rates of different SN types are best done with well-controlled and analyzed SN search data [57–60]. Here we are interested in the realized numbers of different transients when followed up blindly by our volume-limited program. Figure 4 shows the fractions we observed. This includes four possible false alarms (i.e., the transient was not confirmed to be a real transient at all but if real was too faint to be a SN),

eight cataclysmic or eruptive variables in a nearby galaxy or within the MW (but along a line of sight toward a nearby galaxy).

As the program was designed to observe all transients which could be young, nearby SNe, some observations were made of objects eventually not fitting those descriptors. SNe 2018evk and 2018ilu were confirmed as a Type II and a Type Ia, respectively, but at redshifts of $z \sim 0.03$ (a distance of ~ 126 Mpc for $H_0 = 73 \text{ km s}^{-1} \text{ Mpc}^{-1}$; [61]). SN 2018evk was separated by only 0.074 arcmin from the nearest galaxy with a redshift listed in the NASA Extragalactic Database (NED) and well within the galaxy light. That galaxy has a spectroscopic redshift reported as 0.008 [62]. SN2018ilu had a reported redshift of 0.007 based on spectroscopic comparisons [35].

Some of our targets turned out to not be SNe, but non-terminal explosions within our own Milky Way galaxy (but along the line of sight to a nearby galaxy) or extragalactic “SN imposters.” In the language used for SNe within the same host galaxy, the luminous red nova (LRN) 2018bwo [42,63] and the luminous blue variable (LBV) 2018htr [46,64] would be siblings [65,66]. AT2019bl was discovered 1.3 arcmin from UGC3658 but is likely within the Milky Way. AT2019bl is well detected in the UVOT images with a very blue color. It was, however, not spectroscopically classified at the time. ZTF imaging shows it to have had a subsequent eruption, suggesting a recurrent nova classification.

AT2018avo was retracted as a false alarm by the discoverer via comments on the TNS page. Three other objects were too faint to be SNe, but the nature of the transient is unknown. Some transient objects were triggered but not observed by Swift. SN2018imf was spectroscopically similar to SNe II 60 days after explosion before the observations began. A ToO request was submitted for AT2019yv [67]. It was too close to the moon to be observed at the time of the ToO submission, and subsequent spectra showed no SN features [68] before Swift observations could begin.

ePesto published a subsequent non-detection of AT2018fes before Swift observations could be scheduled, so the ToO was withdrawn. SN 2018get was classified as an old IIP and observations dropped.

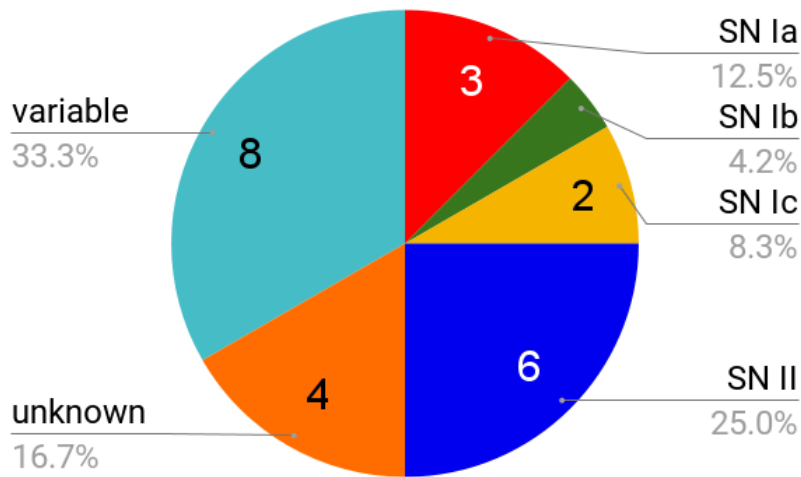


Figure 4. Fractions of transients triggered through this program, including four SNe Ia, one Ca-rich Ib, two SNe Ic, 6 SNe II (including one 87A-like II), eight cataclysmic or eruptive variables, and four reported transients that were too faint to be SNe but the nature of which was not confirmed.

3. Analysis and Results

3.1. UVOT Analysis

Swift/UVOT observations were made in the six medium-band filters. Observations were analyzed using the pipeline of the Swift Optical/Ultraviolet Supernova Archive (SOUSA; [69]). Zeropoints are from Breeveld et al. [70] with the sensitivity correction updated in Sep 2020 and aperture corrections computed using observations from 2018.

UVOT light curves will be posted to the Swift supernova website² and the fits images to the Mikulski Archive for Space Telescopes (MAST)³. Figure 5 shows the UVOT light curves in the *uvw1* filter for our targeted SNe.

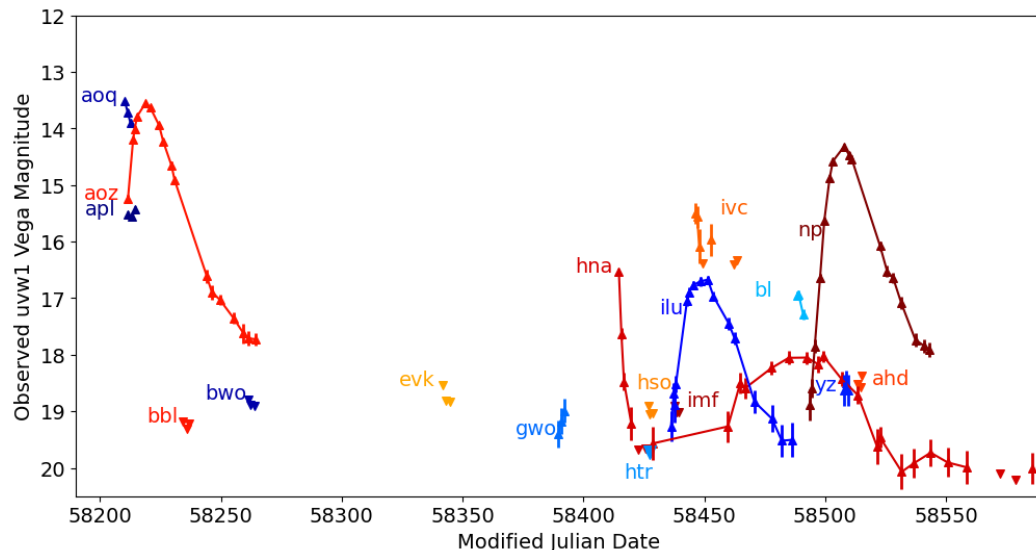


Figure 5. *uvw1*-band light curves of all transients triggered under our program. Only the first three observations of each transient were requested through this program. Follow-up requests obtained the later points. Detections are plotted with upward-facing triangles, and upper limits are plotted with downward-facing triangles.

3.2. XRT Analysis

The SN targets from this program were searched for by name, coordinates, and target ID using the online XRT pipeline⁴. The resulting downloaded data files included values for the observation date and time, count rate or upper limit, and count rate uncertainties. The uncertainties and limits are 95% confidence intervals determined using the method of Kraft et al. [71].

Three supernovae were detected by the pipeline at a statistically significant level: SNe 2018aoq, 2018ivc, and 2018lei. Upon visual examination of the X-ray data, the area near SN 2018aoq has significant X-ray counts from the host galaxy. However, the X-ray counts are not concentrated at the SN location and appear similar to pre-explosion imaging by XRT. The XRT pipeline for the observations of SN 2018lei detects a source at a position of 02 h 33 m 34.25 s, -39 d 02 m 42.5 s. This is 3.3 arcsec from the SN position and 0.7 arcsec from the galaxy center. A source is also detected at a consistent position in the late-time images. Therefore we conclude that the XRT detections of SNe 2018aoq and 2018lei are false detections arising from host galaxy X-ray flux.

A possible X-ray excess is seen at the location of SN 2018ivc compared to pre-explosion images. The automated extraction, however, shows a large scatter in the observed count rates before and after the SN explosion due to flux from the host galaxy [72]. SN 2018ivc was later observed by Chandra and significantly detected at a flux level of 1×10^{40} erg s⁻¹ [73]. It might be possible to use the Chandra observations to subtract constant X-ray sources and recover an earlier X-ray flux from SN 2018ivc.

The remaining, uncontaminated SNe were not detected. Converting observed count rates (or limits) into an integrated X-ray flux or luminosity limit requires a spectral model. Since the X-ray spectrum cannot be constrained from our non-detections, we converted the count rates (or upper limits) to fluxes using an average flux/count rate factor from tabulated values in Immler et al. [6]. These assumed a thermal spectrum of $kT = 10$ eV [74]. The flux limits were converted to luminosity limits using the distances in Table 2. The 0.2–10 keV flux and luminosity limits for the first three epochs of each uncontaminated SN

are printed in Table 3, with the other epochs available in the Supernova X-ray database SNaX [75]. The false alarms and galactic transients are not reported in the table.

Table 2. Host Galaxy Information.

Name	Host Galaxy ^a	Ref. ^b	Type	Dist. Method	Dist. Mod. (mag)	Ref. ^c
SN2018aoq	NGC4151	[76]	II	Dust parallax	31.39 ± 0.28	[77]
AT2018apl	(ESO325-G11)	[78,79]	star/LRN			
SN2018aoz	NGC3923	[80]	Ia	SBF	31.64 ± 0.14	[81]
AT2018avo	(NGC4203)		false alarm			
SN2018bbl	NGC7421	[82]	II	Tully–Fisher	32.2 ± 0.13	[83]
AT2018bsk	(NGC4454)		unconfirmed			
AT2018bvt	(IC3225)		faint			
AT2018bwo	NGC45	[63]	LRN	TRGB	29.16 ± 0.36	[84]
SN2018evk	AnonHost	[85]	II old			
SN2018gwo	NGC4128	[86]	Ib-Ca-rich	Tully–Fisher	32.21 ± 0.45	[87]
SN2018hna	UGC7534	[88]	II-87A	Tully–Fisher	30.11	[89]
AT2018hrq	(NGC404)	[90]	nova			
AT2018hso	NGC3729	[91]	LRN	Tully–Fisher	31.62 ± 0.35	[92]
AT2018htr	NGC45	[64]	LBV	TRGB	29.16 ± 0.36	[84]
SN2018imf	VCC1931	[93]	II			
SN2018ilu	AnonHost	[35]	Ia			
SN2018ivc	M77	[94]	II	Tully–Fisher	30.02 ± 0.39	[95]
SN2018lei	NGC986	[96]	Ic	Tully–Fisher	30.22	[97]
AT2019bl	(UGC3658)		CV			
SN2019np	NGC3254	[98]	Ia	Tully–Fisher	32.58 ± 0.45	[99]
SN2019yz	UGC9977	[100]	Ic	Tully–Fisher	32.18 ± 0.45	[99]
AT2019abn	M51	[101]	ILRT	SBF	29.32 ± 0.14	[81]
AT2019ahd	NGC3423	[102]	LBV			
AT2019clr	(IC4182)		unconfirmed			

^a Galaxies names in parenthesis were the presumed host galaxies of transients which turned out to be Galactic or were not confirmed as real transients. ^b Transient classification reference. ^c Host galaxy distance reference.

Table 3. X-ray 95% Confidence Upper Limits

SN Name	MJD (days)	Days Since Explosion	Exposure (seconds)	Flux Limit ($\text{erg s}^{-1} \text{cm}^{-2} \text{Å}^{-1}$)	Lum Limit (erg s^{-1})
2018aoz	58,211	1.58	727.1	9.61×10^{13}	5.21×10^{40}
2018aoz	58,213	3.71	1889.9	3.71×10^{13}	2.01×10^{40}
2018aoz	58,214	4.34	2993.6	2.40×10^{13}	1.30×10^{40}
2018aoz	58,215	5.38	2755.5	2.45×10^{13}	1.33×10^{40}
2018bbl	58,234	2.17	2988.7	2.28×10^{13}	2.07×10^{40}
2018bbl	58,235	3.93	3088.2	1.47×10^{13}	1.34×10^{40}
2018bbl	58,236	4.76	2393.3	2.65×10^{13}	2.40×10^{40}
2018gwo	58,389	0.77	2933.4	2.63×10^{13}	2.41×10^{40}
2018gwo	58,390	1.74	2988.7	1.81×10^{13}	1.66×10^{40}
2018gwo	58,391	2.99	2986.1	1.71×10^{13}	1.56×10^{40}
2018hna	58,414	1.70	2911.0	2.11×10^{13}	2.79×10^{39}
2018hna	58,415	2.74	2923.5	2.20×10^{13}	2.91×10^{39}
2018hna	58,416	3.80	2725.0	2.19×10^{13}	2.90×10^{39}
2019np	58,493	1.70	2494.8	1.98×10^{13}	2.55×10^{40}
2019np	58,494	2.47	2653.9	8.31×10^{13}	1.07×10^{41}
2019np	58,495	3.73	2539.9	2.40×10^{13}	3.09×10^{40}
2019yz	58,507	4.76	2988.7	2.08×10^{13}	1.85×10^{40}
2019yz	58,508	5.50	2933.5	3.10×10^{13}	2.76×10^{40}
2019yz	58,509	6.68	2990.3	2.63×10^{13}	2.34×10^{40}

The X-ray flux and luminosity limits are plotted in Figure 6. The plots extend to 15 days after the estimated explosion date to include Swift XRT detections of SN 2011dh obtained from the pipeline and Swift XRT and Chandra X-ray measurements of SNe 2008D and 2011dh from Soderberg et al. [12] and Campana and Immler [103]. The early emission of SN 2006aj (aka GRB060218) is much more luminous than our limits, demonstrating that rapid Swift follow-up of ground-discovered SNe can constrain similar emission levels

and rule out afterglow-like X-ray luminosity from the SNe in our sample. The fainter luminosities of SNe 2011dh, 2006bp, and 2008D are harder to constrain for the more distant SNe of even our nearby sample, requiring more sensitivity. Observations to constrain the X-ray luminosity will require deeper Swift observations or the higher sensitivities of Chandra or XMM-Newton, even at the relatively low distance to this sample. The angular resolution to resolve sources from others in the host galaxy is also valuable.

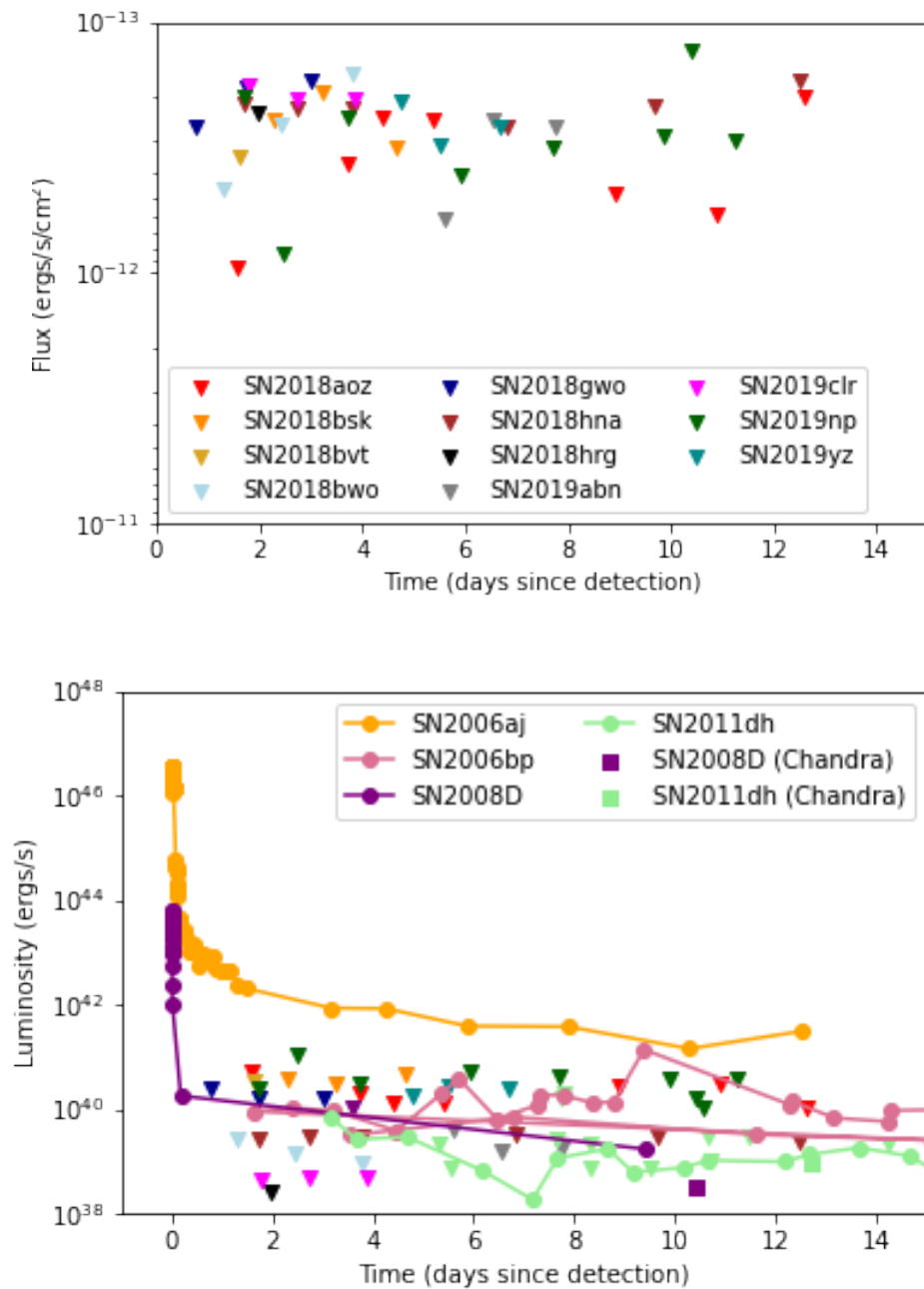


Figure 6. Top panel: X-ray flux limits for the SN sample are shown as downward-pointing arrows. Bottom panel: X-ray luminosity limits from this program (plotted as downward-facing triangles) compared to X-ray detections from previously detected SNe. The limits from this program are more sensitive than the detected luminosity of GRB060218/SN2006aj [11], plotted in yellow circles, allowing us to rule out similar emissions. The Type II SN 2006bp and the Type IIb SN 2011dh had detections of comparable luminosity to the limits measured here.

3.3. Early Observations of SNe Ia

The three SNe Ia observed under this program began about 17, 13, and 10 days before the time of maximum light in the B band. The average rise time after explosion is 18.9 days [104]. Figure 7 compares normalized *b*- and *uvw1*-band light curves of these three SNe Ia with those fit in Devarakonda and Brown [105]. For SN 2018aoz the first Swift observation began about 6 days after the explosion date estimated by Ni et al. [106], while the light curves show one of the shortest rise times from explosion to peak. SN 2019np was observed extremely young. The earliest observations (close to the detection limit) occurred very close to or even before the estimates for the explosion date or first light time calculated by Sai et al. [107]. The sample from this program is not large enough to constrain companion interactions of the broader SN Ia population (but see [106,107] for the individual results), but the method of triggering new transients results in observations closer to the time of explosion.

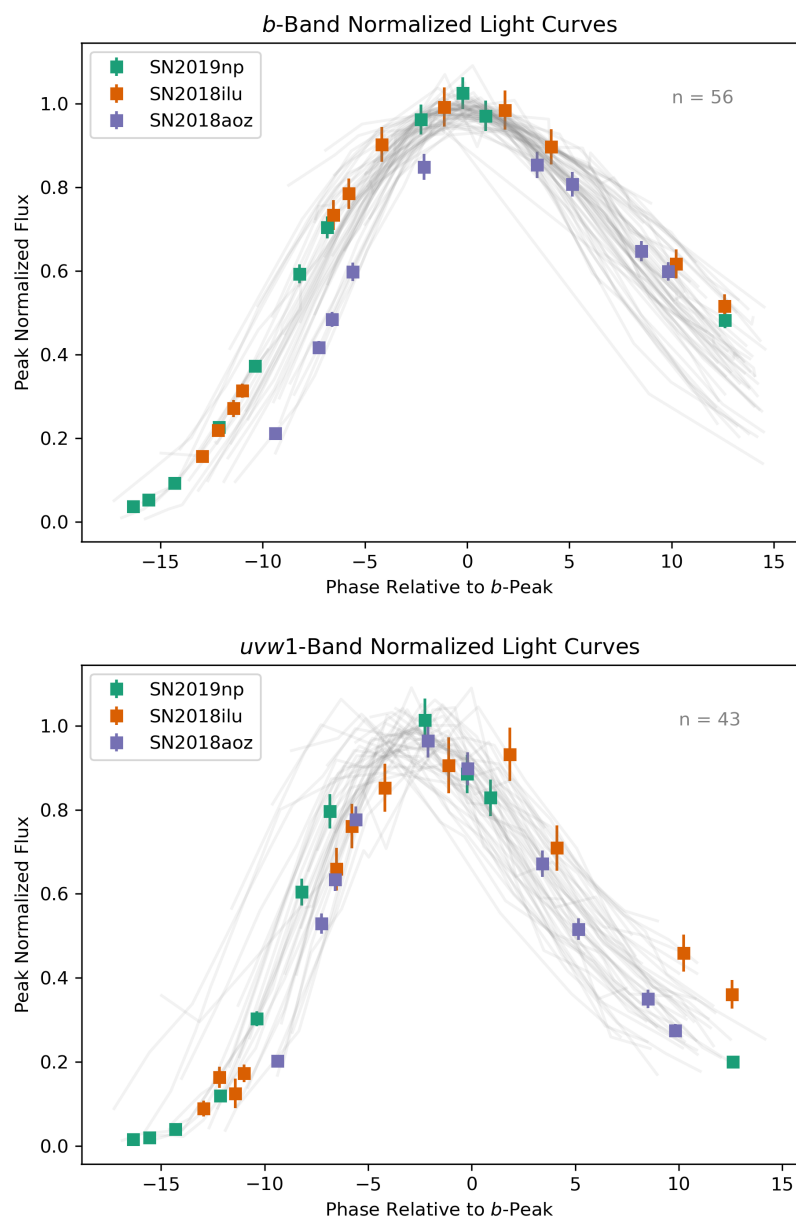


Figure 7. **Top panel:** *b*-band observations of our SNe Ia compared to other UVOT SNe Ia from Devarakonda and Brown [105]. Note the shorter rise time of SN2018aoz. **Bottom panel:** *uvw1*-band observations of our SNe Ia sample.

3.4. SN 2018hna—A SN 1987A Look-Alike

One early goal of the Swift supernova program was to obtain UVOT light curves of at least one example from each SN type. The increase in the number of SNe discovered each year and followed up at a range of different wavelengths has led to a proliferation of SN types [108–110]. One known class not previously observed by Swift was the peculiar Type II class of objects resembling SN 1987A [111]. These are challenging to target because their spectra look similar to normal SNe IIP. Once the photometric signature of an early fading followed by a later re-brightening is observed, it would be too late to observe that fading phase.

By triggering immediately, early data were obtained for SN 2018hna long before their peculiarity was noted by Prentice et al. [112]. The only detections of the early light curve in the mid-UV *uvw2* and *uvm2* filters were during the first two of the three observations from this program.

Figure 8 shows the Swift UVOT light curves of SN 2018hna. Overplotted are light curves of SN 1987A created from generating spectrophotometry in the UVOT system from the IUE spectra of SN 1987A [111]. The apparent magnitudes have been corrected for their relative distance. No extinction corrections or additional shifts have been made. Although some color differences exist, the SNe have very similar luminosities and light curve shapes in the UV and optical.

Singh et al. [113] modeled the light curves to constrain the progenitor star to a radius of ~50 solar radii and 14–20 solar masses. The progenitor of SN2018hna is thus similar to the progenitor of SN1987A.

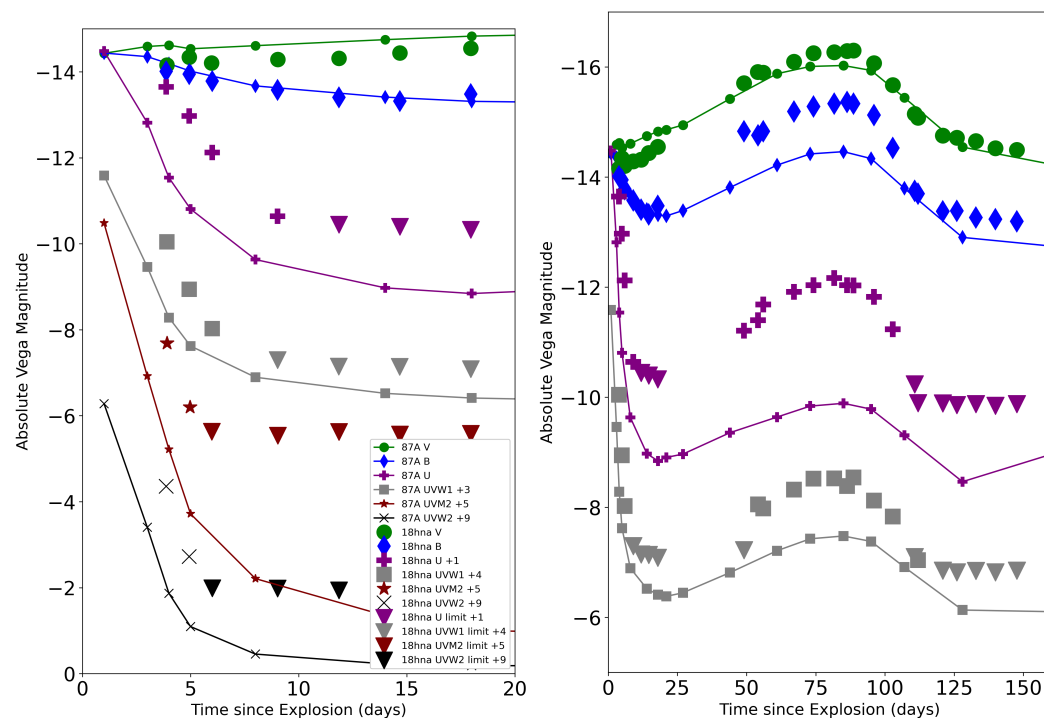


Figure 8. **Left panel:** Swift/UVOT photometry of SN 2018hna (large points) compared to the UVOT spectrophotometry on the IUE spectra of SN 1987A (connected small points) over the first 20 days after explosion. After 2–4 observations the UV flux of SN 2018hna drops below Swift’s limiting magnitude in the u and UV filters. The upper limits are plotted as downward-facing triangles. **Right panel:** Full UVOT light curves in the *uvw1*, *u*, *b*, and *v* of SN 2018hna compared to spectrophotometry of SN 1987A [111] using the same symbols. The UVOT light curves resume 40 days after explosion after reports of the radioactivity-powered re-brightening.

4. Summary and Discussion

This Swift GI key project promptly requested Swift observations of newly discovered, likely extragalactic transients within 35 Mpc without waiting for a spectroscopic classification. The median and average delay times from the discovery image to Swift observation were 1.4 and 2 days. Of the real extragalactic transients observed, highlights include three very young SNe Ia and the early shock cooling from the first 1987A-like SN observed with Swift.

Half of the objects for which we requested Swift observations turned out to be galactic or extragalactic SN “imposters” or possible false alarms. These transients are expected, as the youngest SNe detectable will necessarily be near the detection limit with faint absolute magnitudes. The fraction of these false positives observed by Swift could be reduced by requiring a confirmation image or a classification spectrum which would always involve a delay in the submission of a ToO. Depending on the timing (as neither the proposer nor the appropriate Swift team member responds when asleep), the delay may or may not increase the time to observation. The scientific benefit of earlier observations is in our opinion worth the cost. Canceling follow-up observations promptly if confirmation images or spectra come up negative, as was the case for some of our targets, would reduce the cost. Joining forces with those interested in galactic transients and SN imposters would increase the scientific benefit of more of the observations [114].

This article quantifies the individual delays from transient discovery to Swift observation and demonstrates the value of Swift observations of new transients. The unique instrumentation and observation planning strategies of Swift have resulted in a relatively short observation delay time (median 1.4 days). Further developments in increasing the cadence of transient searches and automating the discovery and announcement steps and the submission to and observation by Swift would further decrease the time between explosion and observation and make the response even swifter. One recent development is the creation of a Swift application which allows for the automated submission of Swift ToOs⁵. With filters to select and submit the appropriate candidates from TNS or transient brokers, automating the submission of Swift ToOs to remove the human from the submission process is a promising route to reduce the time to the first observation. Observing the very moment of explosion for samples of supernovae will require larger-field-of-view UV and X-ray observatories.

Author Contributions: Conceptualization, P.J.B.; methodology, P.J.B.; software, P.J.B.; formal analysis, P.J.B., M.R., E.S. and Y.D.; data curation, P.J.B.; writing—original draft preparation, P.J.B.; writing—review and editing, P.J.B. and M.D.S.; visualization, P.J.B., M.R. and Y.D.; supervision, P.J.B.; funding acquisition, P.J.B., D.P. and M.D.S. All authors have read and agreed to the published version of the manuscript.

Funding: This research was primarily funded by NASA ROSES Swift GI grant 80NSSC19K0316, “Supernova Key Project: Swift Response to New Transients.” Work on SN 2018hna was supported by NASA ADAP grant NNX17AF43G and the updated UVOT photometry by NASA ADAP grant 80NSSC20K0456.

Data Availability Statement: Raw data are available through NASA’s HEASARC. Our final light curves are available via the Swift Supernova Website⁶. Curated image files will be available via the Swift Optical Ultraviolet Supernova Archive (SOUA) on MAST⁷.

Acknowledgments: This work made use of data supplied by the UK Swift Science Data Centre at the University of Leicester. UV data were obtained from the HEASARC and analyzed with the HEASOFT packages.

Conflicts of Interest: The authors declare no conflict of interest.

Abbreviations

The following abbreviations are used in this manuscript:

DOAJ	Directory of open access journals
MAST	Mikulski Archive for Space Telescopes
SOUSA	Swift Optical Ultraviolet Supernova Archive
UVOT	Ultraviolet Optical Telescope
XRT	X-Ray Telescope
SN	Supernova

Notes

- 1 <https://www.wis-tns.org>.
- 2 <https://pbrown801.github.io/SOUSA/>.
- 3 <https://archive.stsci.edu/prepds/sousa/>.
- 4 https://www.swift.ac.uk/user_objects/.
- 5 https://www.swift.psu.edu/too_api/.
- 6 <https://pbrown801.github.io/SOUSA/>.
- 7 <https://archive.stsci.edu/prepds/sousa/>.

References

1. Gehrels, N.; Chincarini, G.; Giommi, P.; Mason, K.O.; Nousek, J.A.; Wells, A.A.; White, N.E.; Barthelmy, S.D.; Burrows, D.N.; Cominsky, L.R.; et al. The Swift Gamma-Ray Burst Mission. *Astrophys. J.* **2004**, *611*, 1005–1020. [[CrossRef](#)]
2. Brown, P.J.; Holland, S.T.; James, C.; Milne, P.; Roming, P.W.A.; Mason, K.O.; Page, K.L.; Beardmore, A.P.; Burrows, D.; Morgan, A.; et al. Ultraviolet, Optical, and X-Ray Observations of the Type Ia Supernova 2005am with Swift. *Astrophys. J.* **2005**, *635*, 1192–1196. [[CrossRef](#)]
3. Brown, P.J.; Baron, E.; Milne, P.; Roming, P.W.A.; Wang, L. Theoretical Clues to the Ultraviolet Diversity of Type Ia Supernovae. *Astrophys. J.* **2015**, *809*, 37. [[CrossRef](#)]
4. Roming, P.W.A.; Kennedy, T.E.; Mason, K.O.; Nousek, J.A.; Ahr, L.; Bingham, R.E.; Broos, P.S.; Carter, M.J.; Hancock, B.K.; Huckle, H.E.; et al. The Swift Ultra-Violet/Optical Telescope. *Space Sci. Rev.* **2005**, *120*, 95–142. [[CrossRef](#)]
5. Burrows, D.N.; Hill, J.E.; Nousek, J.A.; Kennea, J.A.; Wells, A.; Osborne, J.P.; Abbey, A.F.; Beardmore, A.; Mukerjee, K.; Short, A.D.T.; et al. The Swift X-Ray Telescope. *Space Sci. Rev.* **2005**, *120*, 165–195. [[CrossRef](#)]
6. Immler, S.; Brown, P.J.; Milne, P.; The, L.S.; Petre, R.; Gehrels, N.; Burrows, D.N.; Nousek, J.A.; Williams, C.L.; Pian, E.; et al. X-Ray Observations of Type Ia Supernovae with Swift: Evidence of Circumstellar Interaction for SN 2005ke. *Astrophys. J.* **2006**, *648*, L119–L122. [[CrossRef](#)]
7. Koss, M.; Immler, S. Using X-ray Emission from Core-Collapse Supernova Shocks to Probe Circumstellar Environments. *AIP Conf. Proc.* **2007**, *937*, 436–439. [[CrossRef](#)]
8. Ofek, E.O.; Fox, D.; Cenko, S.B.; Sullivan, M.; Gnat, O.; Frail, D.A.; Horesh, A.; Corsi, A.; Quimby, R.M.; Gehrels, N.; et al. X-Ray Emission from Supernovae in Dense Circumstellar Matter Environments: A Search for Collisionless Shocks. *Astrophys. J.* **2013**, *763*, 42. [[CrossRef](#)]
9. Margutti, R.; Milisavljevic, D.; Soderberg, A.M.; Chornock, R.; Zauderer, B.A.; Murase, K.; Guidorzi, C.; Sanders, N.E.; Kuin, P.; Fransson, C.; et al. A Panchromatic View of the Restless SN 2009ip Reveals the Explosive Ejection of a Massive Star Envelope. *Astrophys. J.* **2014**, *780*, 21. [[CrossRef](#)]
10. Pooley, D. X-rays from Core-collapse Supernovae. *Proc. Int. Astron. Union* **2014**, *96*, 103–107. [[CrossRef](#)]
11. Campana, S.; Mangano, V.; Blustin, A.J.; Brown, P.; Burrows, D.N.; Chincarini, G.; Cummings, J.R.; Cusumano, G.; Della Valle, M.; Malesani, D.; et al. The association of GRB 060218 with a supernova and the evolution of the shock wave. *Nature* **2006**, *442*, 1008–1010. [[CrossRef](#)] [[PubMed](#)]
12. Soderberg, A.M.; Berger, E.; Page, K.L.; Schady, P.; Parrent, J.; Pooley, D.; Wang, X.Y.; Ofek, E.O.; Cucchiara, A.; Rau, A.; et al. An extremely luminous X-ray outburst at the birth of a supernova. *Nature* **2008**, *453*, 469–474. [[CrossRef](#)] [[PubMed](#)]
13. Brown, P.J.; Roming, P.W.A.; Milne, P.A. The first ten years of Swift supernovae. *J. High Energy Astrophys.* **2015**, *7*, 111–116. [[CrossRef](#)]
14. Law, N.M.; Kulkarni, S.R.; Dekany, R.G.; Ofek, E.O.; Quimby, R.M.; Nugent, P.E.; Surace, J.; Grillmair, C.C.; Bloom, J.S.; Kasliwal, M.M.; et al. The Palomar Transient Factory: System Overview, Performance, and First Results. *Publ. Astron. Soc. Pac.* **2009**, *121*, 1395. [[CrossRef](#)]
15. Rau, A.; Kulkarni, S.R.; Law, N.M.; Bloom, J.S.; Ciardi, D.; Djorgovski, G.S.; Fox, D.B.; Gal-Yam, A.; Grillmair, C.C.; Kasliwal, M.M.; et al. Exploring the Optical Transient Sky with the Palomar Transient Factory. *Publ. Astron. Soc. Pac.* **2009**, *121*, 1334. [[CrossRef](#)]

16. Kochanek, C.S.; Shappee, B.J.; Stanek, K.Z.; Holoiien, T.W.S.; Thompson, T.A.; Prieto, J.L.; Dong, S.; Shields, J.V.; Will, D.; Britt, C.; et al. The All-Sky Automated Survey for Supernovae (ASAS-SN) Light Curve Server v1.0. *Publ. Astron. Soc. Pac.* **2017**, *129*, 104502. [[CrossRef](#)]
17. Tonry, J.L.; Denneau, L.; Heinze, A.N.; Stalder, B.; Smith, K.W.; Smartt, S.J.; Stubbs, C.W.; Weiland, H.J.; Rest, A. ATLAS: A High-cadence All-sky Survey System. *Publ. Astron. Soc. Pac.* **2018**, *130*, 064505. [[CrossRef](#)]
18. Tartaglia, L.; Sand, D.J.; Valenti, S.; Wyatt, S.; Anderson, J.P.; Arcavi, I.; Ashall, C.; Botticella, M.T.; Cartier, R.; Chen, T.W.; et al. The Early Detection and Follow-up of the Highly Obscured Type II Supernova 2016ija/DLT16am. *Astrophys. J.* **2018**, *853*, 62. [[CrossRef](#)]
19. Drake, A.J.; Djorgovski, S.G.; Mahabal, A.; Beshore, E.; Larson, S.; Graham, M.J.; Williams, R.; Christensen, E.; Catelan, M.; Boattini, A.; et al. First Results from the Catalina Real-Time Transient Survey. *Astrophys. J.* **2009**, *696*, 870–884. [[CrossRef](#)]
20. Hodgkin, S.T.; Harrison, D.L.; Breedt, E.; Wevers, T.; Rixon, G.; Delgado, A.; Yoldas, A.; Kostrzewa-Rutkowska, Z.; Wyrzykowski, Ł.; van Leeuwen, M.; et al. Gaia Early Data Release 3. Gaia photometric science alerts. *Astron. Astrophys.* **2021**, *652*, A76. [[CrossRef](#)]
21. Jones, D.O.; Foley, R.J.; Narayan, G.; Hjorth, J.; Huber, M.E.; Aleo, P.D.; Alexander, K.D.; Angus, C.R.; Auchettl, K.; Baldassare, V.F.; et al. The Young Supernova Experiment: Survey Goals, Overview, and Operations. *Astrophys. J.* **2021**, *908*, 143. [[CrossRef](#)]
22. Bellm, E.C.; Kulkarni, S.R.; Graham, M.J.; Dekany, R.; Smith, R.M.; Riddle, R.; Masci, F.J.; Helou, G.; Prince, T.A.; Adams, S.M.; et al. The Zwicky Transient Facility: System Overview, Performance, and First Results. *Publ. Astron. Soc. Pac.* **2019**, *131*, 018002. [[CrossRef](#)]
23. Wiggins, P. Transient Discovery Report for 2018-09-28. *Transient Name Serv. Discov. Rep.* **2018**, *1459*, 1.
24. Itagaki, K. Transient Discovery Report for 2018-10-22. *Transient Name Serv. Discov. Rep.* **2018**, *1614*, 1.
25. Camarasa, J. Transient Discovery Report for 2018-04-17. *Transient Name Serv. Discov. Rep.* **2018**, *503*, 1.
26. Shappee, B.J.; Piro, A.L.; Holoiien, T.W.S.; Prieto, J.L.; Contreras, C.; Itagaki, K.; Burns, C.R.; Kochanek, C.S.; Stanek, K.Z.; Alper, E.; et al. The Young and Bright Type Ia Supernova ASASSN-14lp: Discovery, Early-time Observations, First-light Time, Distance to NGC 4666, and Progenitor Constraints. *Astrophys. J.* **2016**, *826*, 144. [[CrossRef](#)]
27. Roming, P.W.A.; Koch, T.S.; Oates, S.R.; Porterfield, B.L.; Vanden Berk, D.E.; Boyd, P.T.; Holland, S.T.; Hoversten, E.A.; Immler, S.; Marshall, F.E.; et al. The First Swift Ultraviolet/Optical Telescope GRB Afterglow Catalog. *Astrophys. J.* **2009**, *690*, 163–188. [[CrossRef](#)]
28. Kasen, D. Seeing the Collision of a Supernova with Its Companion Star. *Astrophys. J.* **2010**, *708*, 1025–1031. [[CrossRef](#)]
29. Brown, P.J.; Dawson, K.S.; Harris, D.W.; Olmstead, M.; Milne, P.; Roming, P.W.A. Constraints on Type Ia Supernova Progenitor Companions from Early Ultraviolet Observations with Swift. *Astrophys. J.* **2012**, *749*, 18. [[CrossRef](#)]
30. Brown, P.J.; Dessart, L.; Holland, S.T.; Immler, S.; Landsman, W.; Blondin, S.; Blustin, A.J.; Breeveld, A.; Dewangan, G.C.; Gehrels, N.; et al. Early Ultraviolet, Optical, and X-Ray Observations of the Type IIP SN 2005cs in M51 with Swift. *Astrophys. J.* **2007**, *659*, 1488–1495. [[CrossRef](#)]
31. Immler, S.; Brown, P.J.; Milne, P.; Dessart, L.; Mazzali, P.A.; Landsman, W.; Gehrels, N.; Petre, R.; Burrows, D.N.; Nousek, J.A.; et al. X-Ray, UV, and Optical Observations of Supernova 2006bp with Swift: Detection of Early X-Ray Emission. *Astrophys. J.* **2007**, *664*, 435–442. [[CrossRef](#)]
32. Brown, P.J.; Dawson, K.S.; de Pasquale, M.; Gronwall, C.; Holland, S.; Immler, S.; Kuin, P.; Mazzali, P.; Milne, P.; Oates, S.; et al. A Swift Look at SN 2011fe: The Earliest Ultraviolet Observations of a Type Ia Supernova. *Astrophys. J.* **2012**, *753*, 22. [[CrossRef](#)]
33. Cao, Y.; Kulkarni, S.R.; Howell, D.A.; Gal-Yam, A.; Kasliwal, M.M.; Valenti, S.; Johansson, J.; Amanullah, R.; Goobar, A.; Sollerman, J.; et al. A strong ultraviolet pulse from a newborn type Ia supernova. *Nature* **2015**, *521*, 328–331. [[CrossRef](#)] [[PubMed](#)]
34. Marion, G.H.; Brown, P.J.; Vinkó, J.; Silverman, J.M.; Sand, D.J.; Challis, P.; Kirshner, R.P.; Wheeler, J.C.; Berlind, P.; Brown, W.R.; et al. SN 2012cg: Evidence for Interaction Between a Normal Type Ia Supernova and a Non-degenerate Binary Companion. *Astrophys. J.* **2016**, *820*, 92. [[CrossRef](#)]
35. Berton, M.; Congiu, E.; Benetti, S.; Yaron, O. ePESSTO Transient Classification Report for 2018-11-15. *Transient Name Serv. Discov. Rep.* **2018**, *2034*, 1.
36. Soler, C.; Zheng, W.; Filippenko, A.V. LOSS Transient Discovery Report for 2018-04-01. *Transient Name Serv. Discov. Rep.* **2018**, *426*, 1.
37. Nicholls, B.; Dong, S.; Stanek, K.Z. ASAS-SN Transient Discovery Report for 2018-04-03. *Transient Name Serv. Discov. Rep.* **2018**, *434*, 1.
38. Valenti, S.; Sand, D.J.; Wyatt, S. DLT40 Transient Discovery Report for 2018-04-02. *Transient Name Serv. Discov. Rep.* **2018**, *428*, 1.
39. Parker, S. BOSS Transient Discovery Report for 2018-04-25. *Transient Name Serv. Discov. Rep.* **2018**, *542*, 1.
40. Mishevskiy, N.; CRTS. SNHunt Transient Discovery Report for 2018-05-16. *Transient Name Serv. Discov. Rep.* **2018**, *650*, 1.
41. Mishevskiy, N. SNHunt Transient Discovery Report for 2018-05-21. *Transient Name Serv. Discov. Rep.* **2018**, *684*, 1.
42. Valenti, S.; Sand, D.J.; Wyatt, S. DLT40 Transient Discovery Report for 2018-05-22. *Transient Name Serv. Discov. Rep.* **2018**, *687*, 1.
43. Tonry, J.; Stalder, B.; Denneau, L.; Heinze, A.; Weiland, H.; Rest, A.; Smith, K.W.; Smartt, S.J.; Young, D.R.; Fulton, M.; et al. ATLAS Transient Discovery Report for 2018-08-10. *Transient Name Serv. Discov. Rep.* **2018**, *1136*, 1.
44. Soler, C.; Zheng, W.; Filippenko, A.V. LOSS Transient Discovery Report for 2018-11-01. *Transient Name Serv. Discov. Rep.* **2018**, *1662*, 1.
45. Fremling, C. ZTF Transient Discovery Report for 2018-11-02. *Transient Name Serv. Discov. Rep.* **2018**, *1674*, 1.

46. Valenti, S.; Sand, D.J.; Wyatt, S. DLT40 Transient Discovery Report for 2018-11-03. *Transient Name Serv. Discov. Rep.* **2018**, 1681, 1.
47. Itagaki, K. Transient Discovery Report for 2018-11-14. *Transient Name Serv. Discov. Rep.* **2018**, 1766, 1.
48. Tonry, J.; Denneau, L.; Heinze, A.; Weiland, H.; Flewelling, H.; Stalder, B.; Rest, A.; Stubbs, C.; Smith, K.W.; Smartt, S.J.; et al. ATLAS Transient Discovery Report for 2018-11-14. *Transient Name Serv. Discov. Rep.* **2018**, 1767, 1.
49. Valenti, S.; Sand, D.J.; Wyatt, S. DLT40 Transient Discovery Report for 2018-11-24. *Transient Name Serv. Discov. Rep.* **2018**, 1816, 1.
50. Stanek, K.Z. ASAS-SN Transient Discovery Report for 2018-12-31. *Transient Name Serv. Discov. Rep.* **2018**, 2010, 1.
51. Tonry, J.; Denneau, L.; Heinze, A.; Weiland, H.; Flewelling, H.; Stalder, B.; Rest, A.; Stubbs, C.; Smith, K.W.; Smartt, S.J.; et al. ATLAS Transient Discovery Report for 2019-01-03. *Transient Name Serv. Discov. Rep.* **2019**, 16, 1.
52. Itagaki, K. Transient Discovery Report for 2019-01-09. *Transient Name Serv. Discov. Rep.* **2019**, 53, 1.
53. Fremling, C. ZTF Transient Discovery Report for 2019-01-23. *Transient Name Serv. Discov. Rep.* **2019**, 131, 1.
54. Nordin, J.; Brinnel, V.; Giomi, M.; Santen, J.V.; Gal-yam, A.; Yaron, O.; Schulze, S. ZTF Transient Discovery Report for 2019-01-25. *Transient Name Serv. Discov. Rep.* **2019**, 141, 1.
55. Tonry, J.; Denneau, L.; Heinze, A.; Weiland, H.; Flewelling, H.; Stalder, B.; Rest, A.; Stubbs, C.; Smith, K.W.; Smartt, S.J.; et al. ATLAS Transient Discovery Report for 2019-01-29. *Transient Name Serv. Discov. Rep.* **2019**, 161, 1.
56. Mishevskiy, N. SNHunt Transient Discovery Report for 2019-03-28. *Transient Name Serv. Discov. Rep.* **2019**, 460, 1.
57. Leaman, J.; Li, W.; Chornock, R.; Filippenko, A.V. Nearby supernova rates from the Lick Observatory Supernova Search—I. The methods and data base. *Mon. Not. R. Astron. Soc.* **2011**, 412, 1419–1440. [[CrossRef](#)]
58. Li, W.; Leaman, J.; Chornock, R.; Filippenko, A.V.; Poznanski, D.; Ganeshalingam, M.; Wang, X.; Modjaz, M.; Jha, S.; Foley, R.J.; et al. Nearby supernova rates from the Lick Observatory Supernova Search-II. The observed luminosity functions and fractions of supernovae in a complete sample. *Mon. Not. R. Astron. Soc.* **2011**, 412, 1441–1472. [[CrossRef](#)]
59. Graur, O.; Bianco, F.B.; Huang, S.; Modjaz, M.; Shivvers, I.; Filippenko, A.V.; Li, W.; Eldridge, J.J. LOSS Revisited. I. Unraveling Correlations Between Supernova Rates and Galaxy Properties, as Measured in a Reanalysis of the Lick Observatory Supernova Search. *Astrophys. J.* **2017**, 837, 120. [[CrossRef](#)]
60. Frohmaier, C.; Sullivan, M.; Nugent, P.E.; Smith, M.; Dimitriadis, G.; Bloom, J.S.; Cenko, S.B.; Kasliwal, M.M.; Kulkarni, S.R.; Maguire, K.; et al. The volumetric rate of normal type Ia supernovae in the local Universe discovered by the Palomar Transient Factory. *Mon. Not. R. Astron. Soc.* **2019**, 486, 2308–2320. [[CrossRef](#)]
61. Riess, A.G.; Yuan, W.; Macri, L.M.; Scolnic, D.; Brout, D.; Casertano, S.; Jones, D.O.; Murakami, Y.; Anand, G.S.; Breuval, L.; et al. A Comprehensive Measurement of the Local Value of the Hubble Constant with $1 \text{ km s}^{-1} \text{ Mpc}^{-1}$ Uncertainty from the Hubble Space Telescope and the SH0ES Team. *Astrophys. J. Lett.* **2022**, 934, L7. [[CrossRef](#)]
62. Hill, G.J.; Nicklas, H.E.; MacQueen, P.J.; Tejada, C.; Cobos Duenas, F.J.; Mitsch, W. Hobby-Eberly Telescope low-resolution spectrograph. In *Optical Astronomical Instrumentation*; D’Odorico, S., Ed.; SPIE: Bellingham, WA, USA, 1998; Volume 3355, pp. 375–386. [[CrossRef](#)]
63. Clark, P.; McBrien, O.; Kankare, E.; Yaron, O.; Knezevic, N. ePESSTO Transient Classification Report for 2018-05-23. *Transient Name Serv. Discov. Rep.* **2018**, 701, 1.
64. Siebert, M.R.; Kilpatrick, C.D.; Rojas-bravo, C.; Foley, R.J.; Hermes, J.J.; Campillay, A. Transient Classification Report for 2018-11-04. *Transient Name Serv. Discov. Rep.* **2018**, 1692, 1.
65. Brown, P.J. SOUSA’s Swift Supernova Siblings. *Proc. Swift 10 Years Discov.* **2015**, 233, 125.
66. Scolnic, D.; Smith, M.; Massiah, A.; Wiseman, P.; Brout, D.; Kessler, R.; Davis, T.M.; Foley, R.J.; Galbany, L.; Hinton, S.R.; et al. Supernova Siblings: Assessing the Consistency of Properties of Type Ia Supernovae that Share the Same Parent Galaxies. *Astrophys. J. Lett.* **2020**, 896, L13. [[CrossRef](#)]
67. Nordin, J.; Brinnel, V.; Giomi, M.; Santen, J.V.; Gal-yam, A.; Yaron, O.; Schulze, S. ZTF Transient Discovery Report for 2019-01-23. *Transient Name Serv. Discov. Rep.* **2019**, 132, 1.
68. Callis, E.; Dong, S.; Fraser, M.; Pastorello, A.; Galindo-guil, F.J. ZTF Transient Discovery Report for 2019-01-23. *Transient Name Serv. Discov. Rep.* **2019**, 160, 1.
69. Brown, P.J.; Breeveld, A.A.; Holland, S.; Kuin, P.; Pritchard, T. SOUSA: the Swift Optical/Ultraviolet Supernova Archive. *Astrophys. Space Sci.* **2014**, 354, 89–96. [[CrossRef](#)]
70. Breeveld, A.A.; Landsman, W.; Holland, S.T.; Roming, P.; Kuin, N.P.M.; Page, M.J. An Updated Ultraviolet Calibration for the Swift/UVOT. *AIP Conf. Proc.* **2011**, 1358, 373–376. [[CrossRef](#)]
71. Kraft, R.P.; Burrows, D.N.; Nousek, J.A. Determination of confidence limits for experiments with low numbers of counts. *Astrophys. J.* **1991**, 374, 344–355. [[CrossRef](#)]
72. Robertson, M. Supernovae X-ray Analysis: From Swift to SIBEX. Undergraduate Honors Thesis, Texas A&M University, College Station, TX, USA, 2022.
73. Bostroem, K.A.; Valenti, S.; Sand, D.J.; Andrews, J.E.; Van Dyk, S.D.; Galbany, L.; Pooley, D.; Amaro, R.C.; Smith, N.; Yang, S.; et al. Discovery and Rapid Follow-up Observations of the Unusual Type II SN 2018ivc in NGC 1068. *Astrophys. J.* **2020**, 895, 31. [[CrossRef](#)]
74. Fransson, C.; Lundqvist, P.; Chevalier, R.A. Circumstellar Interaction in SN 1993J. *Astrophys. J.* **1996**, 461, 993. [[CrossRef](#)]
75. Dwarkadas, V.V. On the lack of X-ray bright Type IIP supernovae. *Mon. Not. R. Astron. Soc.* **2014**, 440, 1917–1924. [[CrossRef](#)]
76. Yamanaka, M. Transient Classification Report for 2018-04-02. *Transient Name Serv. Discov. Rep.* **2018**, 432, 1.

77. Hönig, S.F.; Watson, D.; Kishimoto, M.; Hjorth, J. A dust-parallax distance of 19 megaparsecs to the supermassive black hole in NGC 4151. *Nature* **2014**, *515*, 528–530. [[CrossRef](#)]
78. Malesani, D.; Rubin, A.; Heintz, K.E.; Leloudas, G.; Yaron, O.; Knezevic, N. ePESSTO Transient Classification Report for 2018-04-06. *Transient Name Serv. Discov. Rep.* **2018**, 450, 1.
79. Pessev, P.; Geier, S. On the Progenitor and Nature of ASASSN-18gq. *Astronomer's Telegr.* **2018**, 11518, 1.
80. Hosseinzadeh, G.; Valenti, S.; Sand, D.; Wyatt, S.; Bostroem, K.A.; Reichart, D.E.; Haislip, J.B.; Kouprianov, V. Global SN Project Transient Classification Report for 2018-04-02. *Transient Name Serv. Discov. Rep.* **2018**, 433, 1.
81. Tully, R.B.; Courtois, H.M.; Dolphin, A.E.; Fisher, J.R.; Héraudeau, P.; Jacobs, B.A.; Karachentsev, I.D.; Makarov, D.; Makarova, L.; Mitronova, S.; et al. Cosmicflows-2: The Data. *Astron. J.* **2013**, *146*, 86. [[CrossRef](#)]
82. Cartier, R.; Denihy, E.; Pastorello, A.; Elias, J.H.; Dunlap, B.; Hermes, J.J.; Briceno, C. Spectroscopic classification of SN 2018bb1 with Goodman at SOAR Telescope. *Astronomer's Telegr.* **2018**, 11585, 1.
83. Bottinelli, L.; Gouguenheim, L.; Paturel, G.; Teerikorpi, P. The Malmquist bias and the value of H zero from the Tully-Fisher relation. *Astron. Astrophys.* **1986**, *156*, 157–171.
84. Sabbi, E.; Calzetti, D.; Ubeda, L.; Adamo, A.; Cignoni, M.; Thilker, D.; Aloisi, A.; Elmegreen, B.G.; Elmegreen, D.M.; Gouliermis, D.A.; et al. The Resolved Stellar Populations in the LEGUS Galaxies1. *Astrophys. J. Suppl.* **2018**, *235*, 23. [[CrossRef](#)]
85. Stein, R.; Callis, E.; Kostrzewa-Rutkowska, Z.; Fraser, M.; Yaron, O. ePESSTO Transient Classification Report for 2018-08-12. *Transient Name Serv. Discov. Rep.* **2018**, 1159, 1.
86. Leadbeater, R. Transient Classification Report for 2018-10-01. *Transient Name Serv. Discov. Rep.* **2018**, 1486, 1.
87. Theureau, G.; Hanski, M.O.; Coudreau, N.; Hallet, N.; Martin, J.M. Kinematics of the Local Universe. XIII. 21-cm line measurements of 452 galaxies with the Nançay radiotelescope, JHK Tully-Fisher relation, and preliminary maps of the peculiar velocity field. *Astron. Astrophys.* **2007**, *465*, 71–85. [[CrossRef](#)]
88. Leadbeater, R. Transient Classification Report for 2018-10-26. *Transient Name Serv. Discov. Rep.* **2018**, 1638, 1.
89. Karachentsev, I.D.; Makarov, D.I.; Kaisina, E.I. Updated Nearby Galaxy Catalog. *Astron. J.* **2013**, *145*, 101. [[CrossRef](#)]
90. Berton, M.; Congiu, E.; Benetti, S.; Yaron, O. ePESSTO Transient Classification Report for 2018-11-03. *Transient Name Serv. Discov. Rep.* **2018**, 1686, 1.
91. Dahiwal, A.; Fremling, C. ZTF Transient Classification Report for 2020-07-24. *Transient Name Serv. Discov. Rep.* **2020**, 2260, 1.
92. Tully, R.B.; Rizzi, L.; Shaya, E.J.; Courtois, H.M.; Makarov, D.I.; Jacobs, B.A. The Extragalactic Distance Database. *Astron. J.* **2009**, *138*, 323–331. [[CrossRef](#)]
93. Yamanaka, M. Transient Classification Report for 2018-11-15. *Transient Name Serv. Discov. Rep.* **2018**, 2035, 1.
94. Yamanaka, M. Transient Classification Report for 2018-11-24. *Transient Name Serv. Discov. Rep.* **2018**, 1818, 1.
95. Nasonova, O.G.; de Freitas Pacheco, J.A.; Karachentsev, I.D. Hubble flow around Fornax cluster of galaxies. *Astron. Astrophys.* **2011**, *532*, A104. [[CrossRef](#)]
96. Tucker, M.A.; Huber, M.E.; Strader, J.; Stakek, K.Z.; Shappee, B.J. SCAT Transient Classification Report for 2019-01-09. *Transient Name Serv. Discov. Rep.* **2019**, 62, 1.
97. Russell, D.G. The H I Line Width/Linear Diameter Relationship as an Independent Test of the Hubble Constant. *Astrophys. J.* **2002**, *565*, 681–695. [[CrossRef](#)]
98. Burke, J.; Arcavi, I.; Hiramatsu, D.; Howell, D.A.; McCully, C.; Valenti, S. Global SN Project Transient Classification Report for 2019-01-10. *Transient Name Serv. Discov. Rep.* **2019**, 71, 1.
99. Tully, R.B.; Courtois, H.M.; Sorce, J.G. Cosmicflows-3. *Astron. J.* **2016**, *152*, 50. [[CrossRef](#)]
100. Burke, J.; Arcavi, I.; Hiramatsu, D.; Howell, D.A.; McCully, C.; Valenti, S. Global SN Project Transient Classification Report for 2019-01-24. *Transient Name Serv. Discov. Rep.* **2019**, 1232, 1.
101. Burke, J.; Howell, D.A.; Arcavi, I.; Hiramatsu, D.; McCully, C.; Valenti, S. Global SN Project Transient Classification Report for 2019-03-05. *Transient Name Serv. Discov. Rep.* **2019**, 328, 1.
102. Jha, S. Transient Classification Report for 2019-01-30. *Transient Name Serv. Discov. Rep.* **2019**, 1237, 1.
103. Campana, S.; Immler, S. XMM-Newton and Swift observations of the Type IIb supernova 2011dh in Messier 51. *Mon. Not. R. Astron. Soc.* **2012**, *427*, L70–L74. [[CrossRef](#)]
104. Miller, A.A.; Yao, Y.; Bulla, M.; Pankow, C.; Bellm, E.C.; Cenko, S.B.; Dekany, R.; Fremling, C.; Graham, M.J.; Kupfer, T.; et al. ZTF Early Observations of Type Ia Supernovae. II. First Light, the Initial Rise, and Time to Reach Maximum Brightness. *Astrophys. J.* **2020**, *902*, 47. [[CrossRef](#)]
105. Devarakonda, Y.; Brown, P.J. Comparisons of Type Ia Supernova Light Curves in the UV and Optical with the Swift Ultraviolet/Optical Telescope. *Astron. J.* **2022**, *163*, 258. [[CrossRef](#)]
106. Ni, Y.Q.; Moon, D.S.; Drout, M.R.; Polin, A.; Sand, D.J.; González-Gaitán, S.; Kim, S.C.; Lee, Y.; Park, H.S.; Howell, D.A.; et al. Infant-phase reddening by surface Fe-peak elements in a normal type Ia supernova. *Nat. Astron.* **2022**, *6*, 568–576. [[CrossRef](#)]
107. Sai, H.; Wang, X.; Elias-Rosa, N.; Yang, Y.; Zhang, J.; Lin, W.; Mo, J.; Piro, A.L.; Zeng, X.; Reguitti, A.; et al. Observations of the very young Type Ia Supernova 2019np with early-excess emission. *Mon. Not. R. Astron. Soc.* **2022**, *514*, 3541–3558. [[CrossRef](#)]
108. Turatto, M. Classification of Supernovae. In *Supernovae and Gamma-Ray Bursters*; Weiler, K., Ed.; Springer: Berlin/Heidelberg, Germany, 2003; Volume 598, pp. 21–36. [[CrossRef](#)]
109. Turatto, M.; Benetti, S.; Pastorello, A. Supernova classes and subclasses. *AIP Conf. Proc.* **2007**, *937*, 187–197. [[CrossRef](#)]

110. Taubenberger, S. The Extremes of Thermonuclear Supernovae. In *Handbook of Supernovae*; Springer International Publishing: Cham, Switzerland, 2017; p. 317; ISBN 978-3-319-21845-8. [[CrossRef](#)]
111. Pun, C.S.J.; Kirshner, R.P.; Sonneborn, G.; Challis, P.; Nassiopoulos, G.; Arquilla, R.; Crenshaw, D.M.; Shrader, C.; Teays, T.; Cassatella, A.; et al. Ultraviolet Observations of SN 1987A with the IUE Satellite. *Astrophys. J. Suppl. Ser.* **1995**, *99*, 223. [[CrossRef](#)]
112. Prentice, S.J.; Smartt, S.J.; Maguire, K.; Smith, K.W.; McCormack, A.; Denneau, L.; Flewelling, H.; Heinze, A.; Tonry, J.; Weiland, H.; et al. ATLAS and Liverpool Telescope observations of the type II SN 2018hna. *Astronomer's Telegr.* **2018**, *12258*, 1.
113. Singh, A.; Sahu, D.K.; Anupama, G.C.; Kumar, B.; Kumar, H.; Yamanaka, M.; Baklanov, P.V.; Tominaga, N.; Blinnikov, S.I.; Maeda, K.; et al. SN 2018hna: 1987A-like Supernova with a Signature of Shock Breakout. *Astrophys. J. Lett.* **2019**, *882*, L15. [[CrossRef](#)]
114. Page, K.L.; Kuin, N.P.M.; Osborne, J.P. Ultraviolet and X-ray Light-Curves of Novae Observed by the Neil Gehrels Swift Observatory. *Universe* **2022**, *8*, 643. [[CrossRef](#)]

Disclaimer/Publisher's Note: The statements, opinions and data contained in all publications are solely those of the individual author(s) and contributor(s) and not of MDPI and/or the editor(s). MDPI and/or the editor(s) disclaim responsibility for any injury to people or property resulting from any ideas, methods, instructions or products referred to in the content.